
Repetitive Control in the Applications of H-Bridge Active Power Filter

Yang Liu*, Guojun Tan

School of Information and Electrical Engineering, China University of Mining and Technology,
Xuzhou 221008, China.

*Corresponding author, e-mail: liuyangebox@126.com, gjtan@cumt.edu.cn

Abstract

In order to improve the deficiency of the traditional repetitive control, a novel control method combining dead beat control and repetitive control in series is proposed to improve the dynamic performance of the control system. A low-pass filter on the delay link of repetitive control is added to solve the contradiction between repetitive control stability and steady-state accuracy, while the compensation link is designed with the combination of leading phase and the low-pass filter to reduce the control object by relying on accurate mathematical model. The control method, on the basis of steady state accuracy, improves the relative speed and compensation accuracy. The feasibility of the proposed method is verified by the experimental design.

Keywords: repetitive control, deadbeat control, active power filter

Copyright © 2013 Universitas Ahmad Dahlan. All rights reserved.

1. Introduction

A large number of power electronic equipment have been applied in the power grid recently for energy saving and efficiency improvement. This equipment always produces a certain harmonic current distribution, leading to distortion on voltage and current of network common coupling point. The generating sources for the harmonic current are divided into two types, *i.e.*, the load generated harmonic current and a harmonic current caused by the power supply. The load generated harmonic currents are caused by the nonlinear, while the bus harmonic current caused by the power supply is resulted from the distortion of the supply voltage. The presence of harmonic currents in the power grid not only results in the additional loss of energy, but also cause abnormal failure in the grid powered devices. Traditional method to manage harmonic is installation of passive filtering device, either filter harmonic or compensate for reactive power; however, there are the inherent disadvantages of the passive filter on tuning, resonance, and stability.

In order to overcome these shortcomings, the method of employing an active filter device as an alternate to passive filter has been developed rapidly. [1-4] For examples, the theories as instantaneous reactive power theory [1], synchronous reference coordinate transformation [2], PI control [3] and repetitive control [4-6] were applied to active power filter. Though these theories effectively suppress harmonic and compensate reactive, they need coordinate transformation for the collected voltage and current in practical applications. Due to complexity of the compensation, a long computing time of the control chip is required, which result in the decline in the dynamic performance of the active power filter [7-12].

Among different methods (cite references here), repetitive control has a wide range of applications because of the accurate tracking of the periodic signal, however, repetitive control design cannot take the advantages of both the stability and dynamic performance at the same time. Here, we focus on improving the APF repetitive control strategy, including (1) to build leading phase for compensation to the low-pass filter and the delay caused by repetitive control and (2) to add deadbeat control for improving the dynamic performance of repetitive control.

2. Mathematical Model of H-Bridge Bridge Active Power Filter

Figure 1 shows the topological structure of H-bridge Bridge Active Power Filter. Grid three-phase voltages are V_{SA}, V_{SB} and V_{SC} ; three-phase currents are i_{SA}, i_{SB} and i_{SC} ; inductance inductors of active power filter and grid connection are L_A, L_B , and L_C ; current flowing through the connections are i_{LA}, i_{LB} and i_{LC} ; H-bridge DC side capacitor voltage is V_{bus} ; and H-bridge IGBT are $S_{x1}, S_{x2}, S_{x3}, S_{x4}$ ($x=A, B, C$).

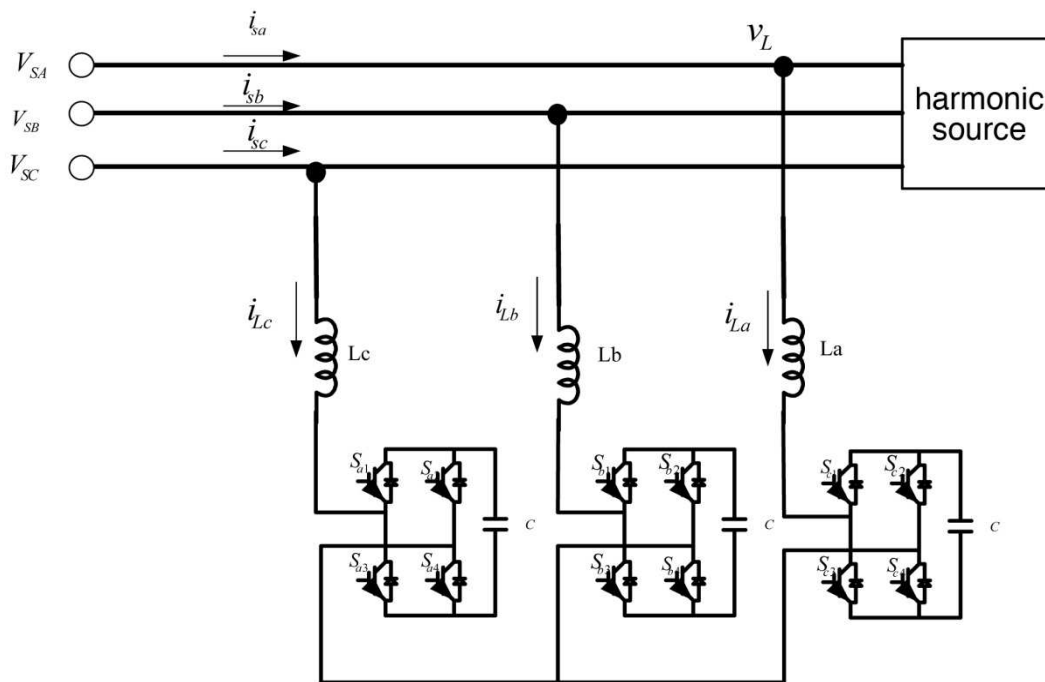


Figure 1. Topological structure of H-bridge Bridge Active Power Filter

In order to establish the mathematical structure model of the H-bridge active power filter, the switch transfer function is defined as:

K_x ($x = a, b, c$)

$$K_x = \begin{cases} = 1 (s_{x1}, s_{x4} \text{ on}) \\ = 0 (s_{x2}, s_{x3} \text{ on}) \end{cases} \quad (1)$$

Voltage across the connection inductance equation is defined as:

$$\begin{aligned} L \frac{di_{La}}{dt} + r \cdot i_{La} &= V_{sa} - V_{bus} \cdot k_a \\ L \frac{di_{Lb}}{dt} + r \cdot i_{Lb} &= V_{sb} - V_{bus} \cdot k_b \\ L \frac{di_{Lc}}{dt} + r \cdot i_{Lc} &= V_{sc} - V_{bus} \cdot k_c \end{aligned} \quad (2)$$

Capacitive current equation is defined as:

$$3C \frac{dV_{bus}}{dt} = \frac{V_{sa} \cdot i_{La} + V_{sb} \cdot i_{Lb} + V_{sc} \cdot i_{Lc}}{V_{bus}} \quad (3)$$

Dodq transformation to equation (2):

$$L \cdot \frac{d}{dt} \left(A \begin{bmatrix} id \\ iq \end{bmatrix} \right) + r \cdot A \begin{bmatrix} id \\ iq \end{bmatrix} = A \begin{bmatrix} vd \\ vq \end{bmatrix} - V_{bus} \cdot A \begin{bmatrix} kd \\ kq \end{bmatrix} \quad (4)$$

Where:

$$A = \begin{bmatrix} \sin(\omega t) & \cos(\omega t) \\ \sin(\omega t - \frac{2}{3}\pi) & \cos(\omega t - \frac{2}{3}\pi) \\ \sin(\omega t + \frac{2}{3}\pi) & \cos(\omega t + \frac{2}{3}\pi) \end{bmatrix}$$

Eliminate A from both sides, and do the Laplace transform, and equation (4) can be written as:

$$\begin{bmatrix} id \\ iq \end{bmatrix} = \frac{1}{Ls + r} \left(\omega L \begin{bmatrix} 0 & 1 \\ -1 & 0 \end{bmatrix} \begin{bmatrix} id \\ iq \end{bmatrix} + \begin{bmatrix} vd \\ vq \end{bmatrix} - V_{bus} \begin{bmatrix} kd \\ kq \end{bmatrix} \right) \quad (5)$$

Namely, current loop model

Because

$$\begin{aligned} V_{sa} \cdot i_{La} + V_{sb} \cdot i_{Lb} + V_{sc} \cdot i_{Lc} &= [V_{sa} \quad V_{sb} \quad V_{sc}] \begin{bmatrix} i_{La} \\ i_{Lb} \\ i_{Lc} \end{bmatrix} = \left(A \begin{bmatrix} vd \\ vq \end{bmatrix} \right)' \left(A \begin{bmatrix} id \\ iq \end{bmatrix} \right) \\ &= [vd \quad vq] A' A \begin{bmatrix} id \\ iq \end{bmatrix} = [vd \quad vq] \begin{bmatrix} 3/2 & 0 \\ 0 & 3/2 \end{bmatrix} \begin{bmatrix} id \\ iq \end{bmatrix} = \frac{3}{2} (vd \cdot id + vq \cdot iq) \end{aligned} \quad (6)$$

Take (6) into (3), and do the Laplace transform, then consider the phase-lockas^{vq = 0}, we obtain voltage loop model,

$$V_{bus} = \frac{1}{C_s} \cdot \frac{vd \cdot id}{2V_{bus}} \quad (7)$$

On the basis of the obtained mathematical model of the active power filter, control strategy is studied. As the repetitive control can achieve accurate compensation, it has been applied in harmonic active power filter. However, the repetitive control cannot take both the stability and dynamic performance into account, the composite controller consisted of deadbeat control and repetitive control improves the system rapidly under the premise of the system accuracy and stability. Improving the repetitive control by combining it with deadbeat control can effectively enhance the performance of active power filter.

3. Composite Control Strategy
3.1. Repetitive Controller Design

The basic structure of general repetitive control is shown in Figure 2 and Figure 3. $E(z)$ is the difference of the reference signal and the output signal. Q is a constant less than 1, or a function having a low-pass nature, which is to ensure the system stable convergence in the entire band. N is the number of samples in each cycle of repetitive control. T_s is the sampling period. $Z = e^{j\omega T_s}$. $G_s(z)$ is the compensation link designed for the control object characteristics, which decides the performance of repetitive control system.

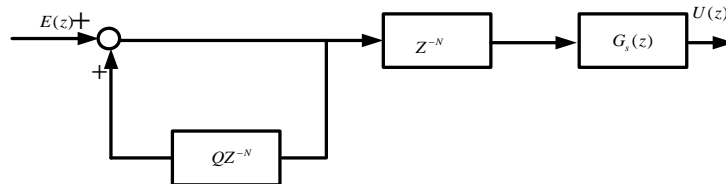


Figure 2. The basic structure of general repetitive control

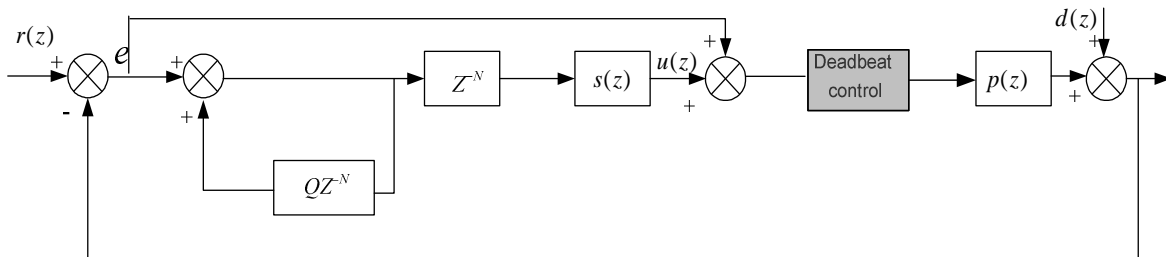


Figure 3. The basic structure of general repetitive control

According to Figure 2 and Figure 3, repetitive control transfer function $G_r(z)$ is

$$G_r(z) = \frac{z^{-N} G_s(z)}{1 - Q(z)z^{-N}} \tag{8}$$

From the transfer function, when the reference signal is the periodic signal, in which angular frequency ω is $2k\pi / T, k \in [0, N/2]$, only the compensation link $G_s(z)$ and the delay link $Q(z)$ influence repetitive control performance.

Figure 3 is the block diagram of active power filter control including deadbeat control. Without deadbeat control, transfer function r to e $G_e(z)$ is as follows:

$$G_e(z) = \frac{e}{r} = \frac{(1 - P)(1 - QZ^{-N})}{1 - Z^{-N}(Q - SP)} \tag{9}$$

The transfer function shows that, when $Q = 1$, $G_e(z) = 0$, the steady-state tracking error of all the harmonics converges to 0; and the system can track the reference signal without steady-state error. As a result, the stability margin of the system can greatly improve when $|Q| < 1$. Therefore, the Q design requires a compromise in stability and steady precision. The Q design has two methods, i.e., to set a constant less than 1 and to design a low-pass filter. In this paper the method of setting a constant less than 1 was employed, while the steady accuracy drop caused by compensator was adjusted.

The equation 9 shows that the pole of system is $Z^N = Q - SP$, static and dynamic characteristics of the system are best when $Z = 0$. Here, the system poles are all in the center of the circle. Correspondingly, $Q = SP$, in ideal intimal case $Q = 1$, when the compensator is designed as $S = P^{-1}$, the system can perform the fastest error convergence and have minimum steady state error. However, this process is heavily dependent on the accurate mathematical model of the controlled object, because undetermined factor and changes in the environment may cause unmolded errors. Moreover, in accordance with $S = P^{-1}$ the design can exist poles outside the unit circle, resulting in the system instability?

In order to eliminate the compensator reliance on accurate mathematical model of the controlled object, the differentiation element is combined herein with the low-pass filter to approximate P^{-1} to get a good compensation performance for

$$S = z^L G_D(z)$$

L is the number of lead compensation steps, $G_D(z)$ is the zero phase low-pass filter.

$$G_D = \frac{\sum_{-D}^0 a_i z^i + \sum_0^D b_i z^i}{\sum_{-D}^0 a_i + \sum_0^D b_i}$$

Wherein the a_i and b_i are filter coefficients, the exponent number of the zero-phase low-pass filter is $2D + 1$, D can be obtained by optimizing design, the goal of optimizing design is

$$MinJ_T = J + \omega D, \omega \in [0, \omega_0], J = \sum_{k=0}^s \mu_k |G_e(z)|, s \text{ is the maximum harmonic number, and } \mu_k \text{ is the weighting coefficients, which can be obtained through experience.}$$

Generated by approximation, z^L is used to compensate for the repetitive control hysteresis. While $G_D(z)$ suppress high frequency interference to the controller.

4. Deadbeat Control

From the examination link to the control link, many calculations of Active Power Filter consume a certain amount of computing time, and cause the decline in dynamic performance of active power filter. As a result, deadbeat control is added to improve the dynamic performance of active power filter.

4.1. Discrete Model of Deadbeat Control

Figure 4 and Figure 5 show a single-phase equivalent circuit of the active power filter, and deadbeat control principle, respectively. The output current of active power filter can be accurately tracked by the reference current within a sampling period.

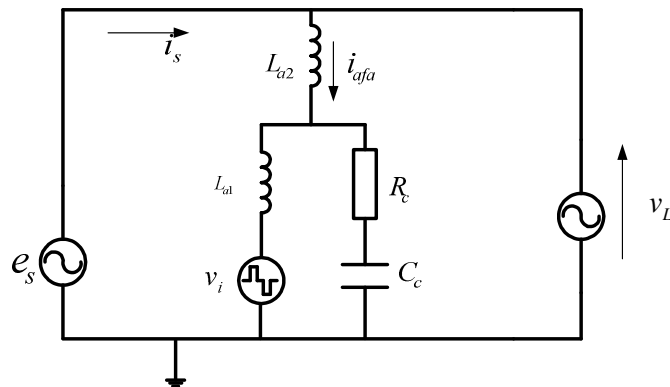


Figure 4. Single-phase equivalent circuit of Active Power Filter

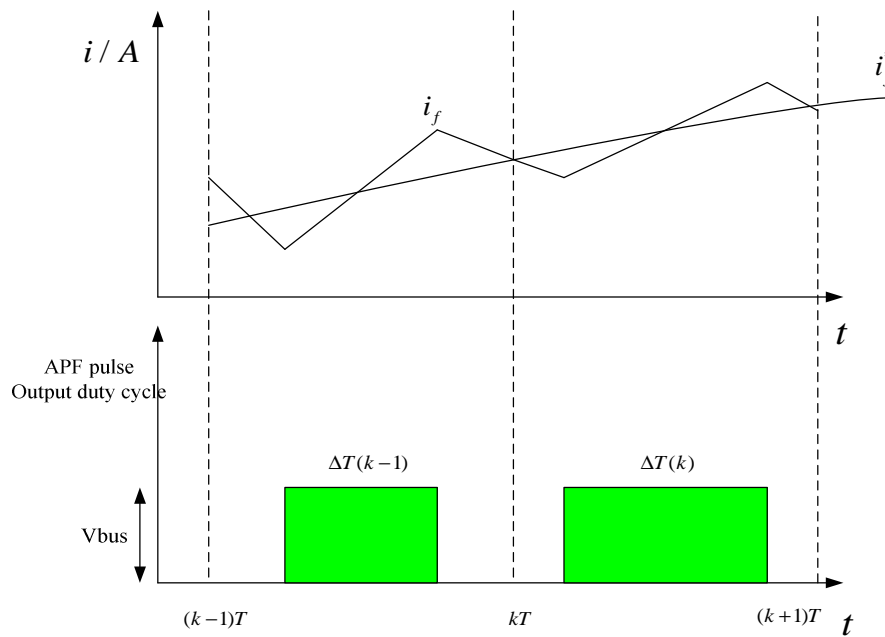


Figure 5. Deadbeat control principle

Through the calculation of detected i_{af}, v_c and i_c , the pulse width of the active power filter is obtained. When i_{af}, v_c and i_c, v_L are determined, a state equation of a single-phase equivalent circuit is obtained according to Figure 4.

$$\begin{aligned} \frac{d}{dt}x &= Ax + bv_i \\ i_{af} &= c^T x \end{aligned} \tag{10}$$

$$A = \begin{bmatrix} -\frac{R_c}{L_{a1}} & -\frac{1}{L_{a1}} & \frac{R_c}{L_{a1}} & 0 \\ \frac{1}{C_c} & 0 & -\frac{1}{C_c} & 0 \\ \frac{R_c}{L_{a2}} & \frac{1}{L_{a2}} & -\frac{R_c}{L_{a2}} & -\frac{1}{L_{a2}} \\ 0 & 0 & 0 & 0 \end{bmatrix} \quad \begin{aligned} x &= [i_c \quad v_c \quad i_{af} \quad v_L]^T \\ b &= [\frac{1}{L_1} \quad 0 \quad 0 \quad 0]^T \\ c &= [0 \quad 0 \quad 1 \quad 0]^T \end{aligned}$$

Discretize equation 8 to obtain equation 9

$$\begin{aligned} x(k+1) &= Fx(k) + g\Delta T(k) \\ i_{af}(k) &= c^T x(k) \end{aligned} \tag{11}$$

$$F = e^{ATs} = \begin{bmatrix} F_{11} & F_{12} & F_{13} & F_{14} \\ F_{21} & F_{22} & F_{23} & F_{24} \\ F_{31} & F_{32} & F_{33} & F_{34} \\ 0 & 0 & 0 & 0 \end{bmatrix} g = e^{\frac{ATs}{2} bV_{bus}} = [g_1 \quad g_2 \quad g_3 \quad 0]^T$$

In which, discrete model of the output current of active power filter is obtained,

$$i_{af}(k+1) = F_{31}i_c(k) + F_{32}v_c(k) + F_{33}i_{af}(k) + F_{34}v_L + g_3\Delta T(k) \quad (12)$$

Wherein the $\Delta T(k)$ is pulse width. When $i_{af}(k+1) = i_{af}^*(k+1)$, it can be obtained by the following equation 13,

$$\Delta T(k) = \frac{i_{af}^*(k+1) - F_{31}i_c(k) - F_{32}v_c(k) - F_{33}i_{af}(k) - F_{34}v_L(k)}{g_3} \quad (13)$$

4.2 State Observer Design

When the observer of state variable x_c is designed, the predictive value of \hat{i}_c and \hat{v}_c can be successfully obtained by equation 12. \hat{x}_c is the predictive value of the state variable x_c .

$$\hat{x}_c(k) = F_c \hat{x}_c(k-1) + F_a \hat{x}_a(k-1) + g_c \Delta T(k-1) - L_c \{i_c(k-1) - c_c^T \hat{x}_c(k-1)\} \quad (14)$$

$$x_c(k) = \begin{bmatrix} i_c(k) \\ v_c(k) \end{bmatrix} x_a(k) = \begin{bmatrix} i_{af}(k) \\ 0 \end{bmatrix} F_c = \begin{bmatrix} F_{11} & F_{12} \\ F_{21} & F_{22} \end{bmatrix} F_a = \begin{bmatrix} F_{13} & F_{14} \\ F_{23} & F_{24} \end{bmatrix}$$

$$g_c = \begin{bmatrix} g_1 \\ g_2 \end{bmatrix} c_c^T = [1 \quad 0] L_c = \begin{bmatrix} l_1 \\ l_2 \end{bmatrix}$$

l_1 and l_2 are observer gain, depending on the stability of the state observer.

v_L and i_{af} is calculated by the equations 12 and 13, respectively.

$$\hat{v}_L(k) = v_L(k-1) + K_v \{v_{Lf}(k) - v_{Lf}(k-1)\} \quad (15)$$

$$\hat{i}_{af}(k) = i_{af}(k-1) \quad (16)$$

Replace $\Delta T(k)$ in the equation 13 with predicted values $\hat{i}_c(k)$, $\hat{v}_c(k)$, $\hat{v}_L(k)$, and $\hat{i}_{af}(k)$:

$$\Delta T(k) = \frac{i_{af}^*(k+1) - F_{31}\hat{i}_c(k) - F_{32}\hat{v}_c(k) - F_{33}\hat{i}_{af}(k) - F_{34}\hat{v}_L(k)}{g_3}$$

5. Experimental

Experiments were carried out in the platform of Active Power Filter with a rated current of 50A and three-phase three-wire 6-pulse rectifier, which produced $17 \pm 0.8 A$ of total harmonic current. The total harmonic current is approximately $1/3$ of the rated current of active power filter. The model of XC3SD1800A Xilinx FPGAs with DSP processing functions was used in the controller; while the power modules of the Infineon Econo Dual packaged IGBT were utilized. The parameters for Active power filter system are shown in Table 1.

Figure 6 is a diagram of the experimental device. In order to better reflect the superiority of the composite control algorithm, two extremes experiments, instantaneous sudden loading and sudden load reduction on active power filter, were selected.

Table 1. The experiment data list for Active power Filter

Parameter	Values of the parameters	Parameter	Values of the parameters
L_s / mH	40	$C_c / \mu F$	5.0
L_{c1} / mH	1.5	$C / \mu F$	5600
L_{c2} / mH	2.0	u_{dc} / V	700
R_c / Ω	10	$T_s / \mu s$	100



Figure 6. The experimental device

Figure 7 is the effect diagram of sudden loading to the stable operation, while Figure 8 is the effect diagram of sudden load reduction to the stable operation. In accordance with the experimental waveforms, Figures 7 and 8 show that response time for APF with deadbeat control is 9ms, which is superior to traditional repetitive control dynamic response time (15ms).

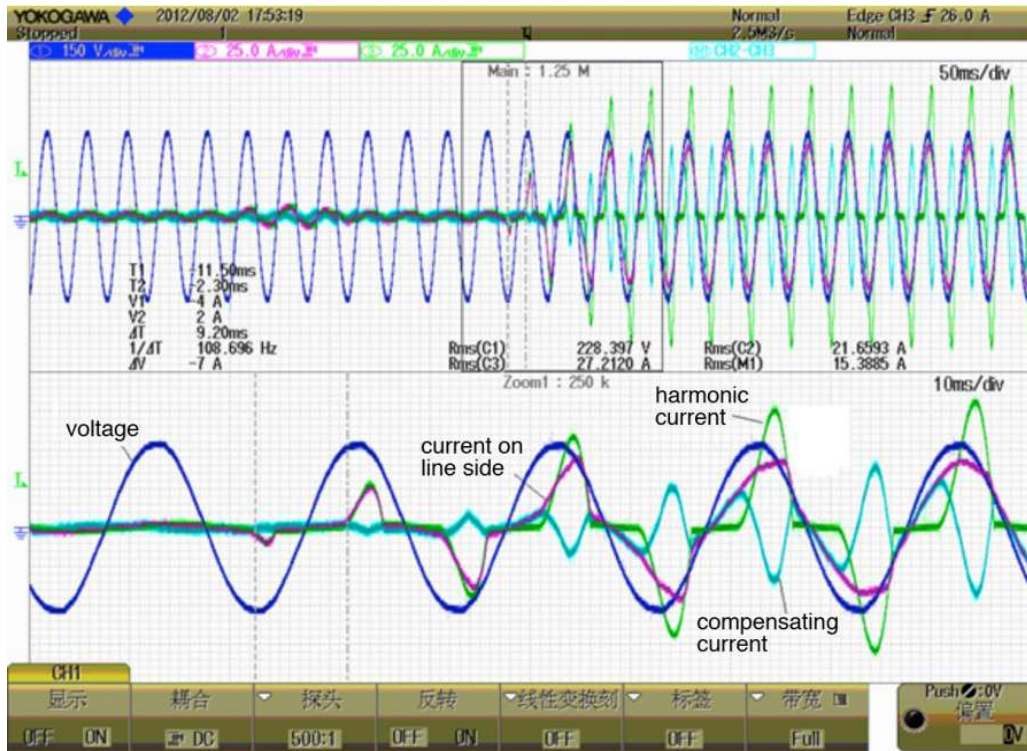


Figure 7. Effect diagram of sudden loading to the stable operation

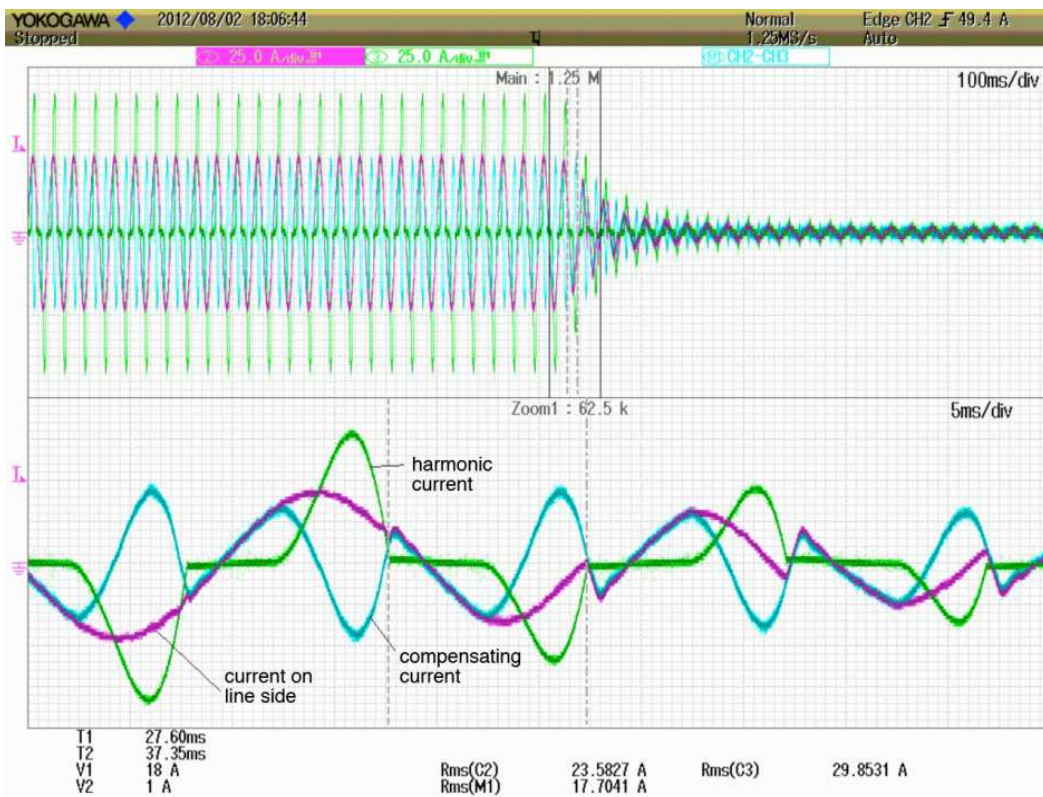


Figure 8. Effect diagram of sudden load reduction to the stable operation

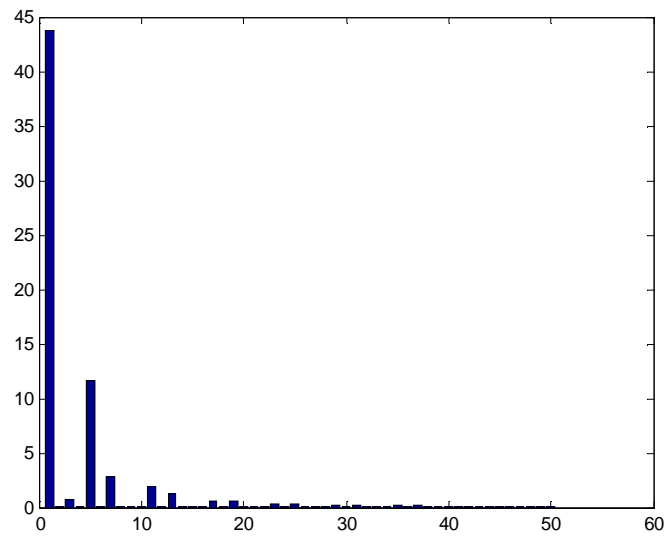


Figure 9. The harmonic histogram of harmonic generated with load

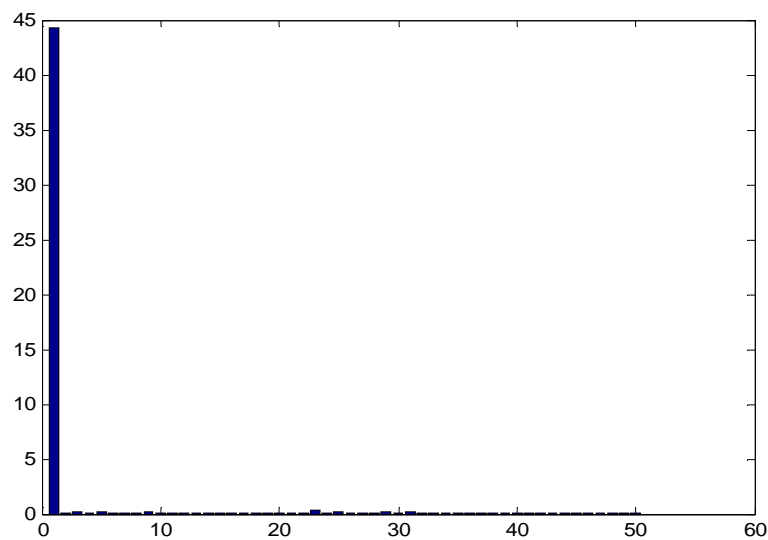


Figure 10. The side harmonic histogram of APF added grid

The FFT transform was performed on the experimental data, in order to quantitatively analyze the compensate effect of complex control algorithm. Figure 9 is the harmonic histogram of harmonic generated with load in system, while Figure 10 is a side harmonic histogram of APF added grid. Through these two histograms, APF is steady in good effect when harmonic distortion ratio is 1.21%. Even when the load is $1/3$, the compensation effect is also good.

6. Conclusion

To sum up, we established a mathematical model of the active power filter with three-phase H-bridge structure, and subsequently studied the reasons why the accuracy and stability of traditional repetitive control cannot be simultaneously satisfied. With the mathematical model of the active power filter, the differentiation element was combined with the low-pass filter to approximate P^{-1} to get a good compensation performance and to solve the problem of the contradiction between repetitive control stability and steady precision. Moreover, deadbeat

control and repetitive control were combined to enhance the dynamic performance of the active power filter and subsequent the system rapidity. Through experimental, it was confirmed that the control method effectively improved the dynamic performance of the active power filter, and, the total harmonic distortion rate were controlled within about 1.2% when load was light.

References

- [1] H Akagi and S Atoh. "Control strategy of active power filter using multiple voltage source PWM converters". IEEE Transactions on Industry Applications. 1986; IA-22: 460-465.
- [2] B Singh, K Al-Haddad, and A Chandra. "A review of active power filters for power quality improvement". IEEE Transaction on Industrial Electronics. 1999; 46(5): 960-971.
- [3] M El-Habrouk, MK Darwish and P Mehta. "Active power filters: A review". IEE Proceedings on Electric Power Applications. 2000; 147(5): 403-413.
- [4] S Hamasaki, M Cao. "Experimental Verification of Disturbance Observer Based Active Filter for Resonance Suppression". IEEE Trans. On Industrial Electronics. 2003; 50(6).
- [5] S Hamasaki, K Fujii, M Tsuji and S Chen. "A Novel Method of Active Filter Control using Repetitive Control". ICEMS2005. 2005; 1252-1256.
- [6] The PROCEEDINGS, Roan, PROCEEDINGS new active filter control delay compensation method. *Transactions of China Electrotechnical Society*. 2008; 23 (11): 166-172.
- [7] Jing Rong, SU Mei, Sun Yao. Improvement of active power filter repetitive control and its optimization design. *Transactions of China Electrotechnical Society*. 2012; 27(2): 236-242.
- [8] Costa-Castello R, Grino R, Fossas E. Odd-harmonic digital repetitive control of a single-phase current active filter. *IEEE Transactions on Power Electronics*. 2004; 19(4): 1060-1068.
- [9] Zhang Bin, Wang Danwei, Zhou Keliang, et al. Linear phase lead compensation repetitive control of a CVCF PWM inverter. *IEEE Transactions on Industrial Electronics*. 2008; 55(4): 1595-1602.
- [10] S Hamasaki, T Kusaba, Y Mazaki. A Novel Method for Active Filter Applying The Deadbeat Control and The Repetitive Control. *Electrical Machines and System*. 2009. ICEMS. 2009: 1-6.
- [11] Han Yang. A Pedagogical Approach for Modeling and Simulation of Switching Mode DC-DC Converters for Power Electronics Course. *TELKOMNIKA Indonesian Journal of Electrical Engineering*. 2012: 10(6).
- [12] Alfonso Fernandez-Vazquez, Gordana Jovanovic Dolecek. On Passband and Stopband CIC Improvements Using a Second Order IIR Filter. *TELKOMNIKA Indonesian Journal of Electrical Engineering*. 2012: 10(1).